IEEE Access
Multidisciplinary | Rapid Review | Open Access Journal

Received July 16, 2019, accepted August 12, 2019, date of publication August 21, 2019, date of current version September 12, 2019.

Digital Object Identifier 10.1109/ACCESS.2019.2936762

Optimal Planning for Partially Self-Sufficient Microgrid With Limited Annual Electricity Exchange With Distribution Grid

QIFANG CHEN[1,2], (Member, IEEE), MINGCHAO XIA[1], (Senior Member, IEEE), YUE ZHOU[2], (Member, IEEE), HANMIN CAI[3], (Member, IEEE), JIANZHONG WU[2], (Member, IEEE), AND HAIBO ZHANG[4], (Member, IEEE)

[1]School of Electrical Engineering, Beijing Jiaotong University, Beijing 100044, China
[2]School of Engineering, Cardiff University, Cardiff CF24 3AA, U.K.
[3]Department of Electrical Engineering, Technical University of Denmark, 2800 Kgs. Lyngby, Denmark
[4]State Key Laboratory of Alternate Electrical Power System with Renewable Energy Sources, North China Electric Power University, Beijing 102206, China

Corresponding author: Mingchao Xia (mchxia@bjtu.edu.cn)

This work was supported in part by the Fundamental Research Funds for the Central Universities under Grant 2018JBM062, in part by the National Science Foundation of China under Grant 51677003, in part by the State Key Laboratory of Alternate Electrical Power System with Renewable Energy Sources under Grant LAPS18018, and in part by the Project Funded by China Postdoctoral Science Foundation under Grant 2018M631326.

ABSTRACT Existing research on on-grid microgrid planning is carried out with a free trading assumption and without considering the limitation of annual electricity exchange. Therefore, the existing planning and sizing scheme may be not viable for the application of partially self-sufficient microgrid (PSSMG) with a limited amount of electricity exchange. To address this issue, a new planning method for PSSMG is proposed in this paper considering the limited annual electricity exchanging amount (AEEA). The sizing model and energy management are linearized and simultaneously integrated into one model, which could be solved in polynomial time. In order to effectively reduce the number of variables of a full year horizon and to cope with the uncertainty both of DGs and loads, a data-driven method based on K-means algorithm is utilized to choose a set of typical days that are representative of historical data of one full year. Finally, the validity and effectiveness of the proposed model are verified by comparative numerical simulations, and the sensitivity of limited AEEA to the planning scheme is analyzed.

INDEX TERMS Microgrid, optimal planning, optimal sizing, data-driven.

I. INTRODUCTION

With the rapid development of Distributed Generation (DG) technology, integration of DG in the end-user side is booming [1]–[3]. Due to its uncertainty and non-schedulable features, it is not suitable to install DGs independently, which would otherwise result in an undesired fluctuation. Therefore, integrating the DGs, loads, and energy storage system (ESS) into a microgrid is one of the most common technological options. It can not only supply stable clean electricity to the end-users and increase the penetration of DGs but also enhance the system reliability with advanced planning and energy management [4], [5]. Depending on its operating mode, a microgrid may be categorized into on-grid microgrid or off-grid microgrid [6], [7]. Also, by its application scenarios, microgrids may be classified into industrial microgrids, commercial microgrids, community microgrids etc. So, different microgrids may have different operation purpose and modes, as well as load profiles. Thus, the types and sizings of DGs may be different from each other, and some specific characteristics need to be thoroughly considered in the planning method. It is clear that a successful implementation of advanced microgrids will require advanced planning strategies to best capture operational and financial benefits. If the internal sources are not properly planned according to the operation purpose of a microgrid, it may affect the performance of microgrid energy management. Thus, it may result in high investment and operation cost at low energy efficiency. So, the optimal planning scheme is the premise of economic operation of a microgrid and many

The associate editor coordinating the review of this article and approving it for publication was Amedeo Andreotti.

endeavors have been conducted on the planning or sizing problem of microgrids [8]–[20].

Since battery storage is of great significance to enhance the power-supply reliability and operational feasibility, a battery optimization model of microgrid planning is studied in [8], [9]. A life cycle planning methodology considering demand growth, battery capacity fading and components' contingencies under a multi-timescale decision framework is studied in [8]. An optimization model for battery storage is proposed to reduce the operation cost and improve the reliability of microgrid in [9], in which some normally overlooked factors of battery are considered in the optimization model. In [10], a reliability-driven DG siting and sizing framework is proposed with the consideration of the existing DGs. An energy index of reliability is presented as the reliability criteria. In [11], an optimal capacity planning method is studied for off-grid remote community microgrids considering the N-1 security constraints. In [12], a comprehensive generalized methodological framework based on the synergies of decision analysis and optimization model is proposed for the design of rural community microgrids. This framework is comprised of three stages, namely, an energy alternative selection, an optimal sizing and an optimal scheme selection. In [13], an optimal planning framework is proposed for the design of low-power low-voltage DC microgrids along with photovoltaic (PV) panels and battery storage. All the researches mentioned above only focus on the planning sub-problem with a deterministic scenario, without considering the uncertainties of DGs or the relation between operation sub-problem and planning sub-problem. The planning stage and operation stage are the two key problems that have intensive interactions. Getting the best profits both in the economy and the stability are their common purposes. So, a joint planning framework is essential to ensure that the operation strategy fit in the planning scheme well. The uncertainty of DGs is one of the important factors that affect the reliable operation of microgrids. So, the uncertainty of DGs should also be taken into consideration during the planning stage. In [14], to cope with the uncertainty associated problem, an optimal planning method based on stochastic programming and Monte Carlo approach is proposed to study the battery capacity expansion for remote microgrids with wind farms. In [15], aiming at maximizing the total profit, a probability-weighted robust optimization method is proposed for microgrids planning over a long-term horizon. The uncertainties of wind turbine (WT) output and loads are modelled as probability-weighted uncertainty sets. In [16], a stochastic programming method is utilized to optimize the investment of energy storage system in microgrids, where the random scenarios of renewable energy generation are considered. To cope with the uncertainties, a chance-constrained information-gap decision model for multi-period microgrid expansion planning is presented in [17]. The investment cost and the operation cost are jointly minimized in the proposed method, but the computational burden is large due to the complex optimization model. In [18], a joint optimal design method for off-grid microgrids considering security constraints is studied. It also points out that techniques based on a probabilistic nonlinear model entail significant computational burdens and cannot sufficiently guarantee the optimality of their solutions, especially when applied to large problems. So, some reasonable simplification steps are presented, such as using some typical days to represent a one-year planning horizon to reduce the number of variables. But the typical days are usually chosen according to human experiences, which may reduce the viability of the planning scheme. Considering load forecast errors, renewable energy generation and electricity market, a robust optimization approach is proposed for microgrid planning in [19]. The planning and operation are jointly considered by decomposing the planning problem into one investment master problem and one operation sub-problem in a sequential way. However, by the sequential calculation model, it may take a dramatic amount of CPU time to simulate over a long period of time for every tested design point generated by the sizing loop [20]. Hence, a design approach aiming at combining the energy management and the sizing model is proposed to reduce the computational time in [20].

From the perspective of methodology, the way to cope with uncertainties and the combination of planning sub-problem and operation sub-problem are the two latest concerns to make the planning scheme more reasonable. However, these two aspects may both increase the complicity of the planning model and result in a significant calculation burden. In this regard, a simplified method to reduce the complicity of the planning model without compromising the validity of the planning scheme is necessary.

From the perspective of the microgrids operation modes, both the researches on on-grid microgrids or off-grid microgrids are conducted. In terms of off-grid microgrids, all loads are supplied by internal sources and energy storage system without other systems to either complement the electricity shortage or absorb the excessive electric power. So, economy and reliability are the two main concerns and many efforts have been contributed to that [21], [22]. With regard to on-grid microgrids, surplus electric power generated by DGs can be fed back to the distribution network and the electricity shortage can be replenished by the distribution network. So, the distribution network is regarded as a free reserve system without limitation in existing literature. However, this will not generally be the case. At first, the system operator will charge a reserve service bill according to the maximum load at the point of common coupling (PCC) or the power rating of the transformer at the connection. This needs to be account for in the planning model. Besides, in order to motivate the development of distributed energy microgrids, some policies are issued by some provinces in China, such as Jiangsu province [23]. According to this policy, the capacity of RESs should be no less than 50% of the maximum load in a microgrid and the annual electricity exchanging amount (AEEA) should be no more than 50% of the annual electricity demand. Thus, the planning model with a limited AEEA and

a minimum capacity limit of RESs is a new challenging problem for on-grid microgrids. Hence, this paper proposes a new planning method to tackle this problem taking into account the newly introduced regulation constraints mentioned above.

The main contributions of this paper are summarized as follows.

1) The proposed planning model integrates the sizing and the optimal operation problems into one model. Also, no sequential interaction loop between the sizing problem and energy management is needed when solving the model, which could substantially reduce the computational burden.
2) Some nonlinear problems are linearized to model the proposed integrated planning model as a linear one so that the optimal planning model could be solved in polynomial time.
3) Unlike conventional ways of choosing typical days by experiences, a data-driven method based on K-means clustering algorithm is used to group the historical data so that the data of typical days could be more representative.
4) The reserve service bill of the distribution network is considered by formulating the capacity of the transformer at the PCC as a decision variable and including in the objective function.

The rest of this paper is organized as follows. In section II is partially self-sufficient microgrid is described in detail. The detailed planning model of the PSSMG is introduced in section III and IV. To validate the proposed method, numerical studies are conducted and summarized in section V. The final conclusion is presented in section VI.

II. DESCRIPTION OF THE PARTIALLY SELF-SUFFICIENT MICROGRIDS

A. SYSTEM STRUCTURE

Consider an on-grid microgrid with a limited AEEA and a minimum capacity limit of RESs. A certain part of electricity demand should be supplied by the DGs in the microgrid. So, this kind of microgrid can be called as partially self-sufficient microgrid (PSSMG), which needs electricity exchange with the distribution network, not entirely self-sufficient. As shown in Fig. 1 is the diagram of system structure. It consists of dispatchable sources (diesel engine (DE) and energy storage system), non-dispatchable sources (WT and PV) and loads. Loads can be classified into controllable loads and uncontrollable loads [24]. In this paper, all loads in MG are assumed to be uncontrollable in the planning model. The electricity between the on-grid microgrid and the distribution network is only exchanged through the PCC. Hence, exchanged power should not exceed the power rating of the transformer at the PCC. In addition, the AEEA should not exceed a certain value (such as 50%) of the annual demand in microgrid either and the capacity of RESs should be larger than a certain value (such as 50%) of the maximum load.

TABLE 1. Definitions of symbols used in section II.

P_{ex}	The exchanging power at the PCC
E_{ex}	The AEEA
$P_{ld}^{\max}$	The maximum load in microgrid
P_{tr}	The power rating of the transformer
E_{an}	The annual electricity demand
$\mathbb{E}_{res}$	The total capacity of RESs
$\mathbb{E}_{pv}$	The capacity of PV
$\mathbb{E}_{wt}$	The capacity of WT

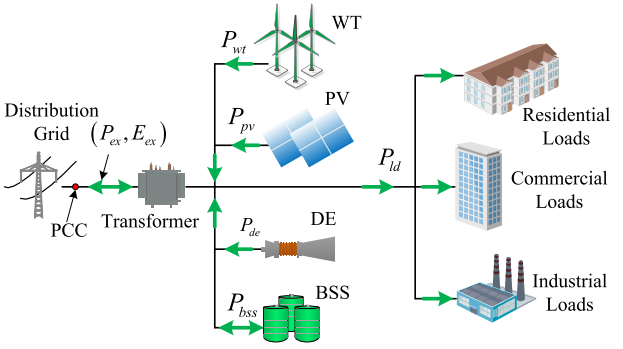

FIGURE 1. The structure of on-grid microgrids.

$$\begin{cases} P_{ex} \le P_{tr} \\ E_{ex} \le \alpha E_{an}, & \alpha \in [0, 1] \\ \mathbb{E}_{res} \ge \beta P_{ld}^{\max}, & \beta \in [0, 1] \\ \mathbb{E}_{res} = \mathbb{E}_{wd} + \mathbb{E}_{pv} \end{cases} \tag{1}$$

where, α, β are constant coefficient.

B. POWER EXCHANGING BETWEEN DISTRIBUTION NETWORK AND MICROGRIDS

For on-grid microgrids, distribution network always works as a reserve system to replenish power shortage and absorb excessive power. It will not only cost system resources to keep on-grid microgrids stable but also need to pay for the electricity fed into the network. In practice, utility operator would charge a reserve service bill according to the reserve capacity, which is proportional to the power rating of the transformer or the maximum load at the PCC. In other words, if the power rating of the transformer and the maximum load at the PCC are small, the reserve service bill would be marginal. However, this would require a high capacity of the internal generation sources leading to an increased investment of microgrids. Furthermore, because of the uncertainties, the high penetration level of DGs would result in high complicity of microgrids control and scheduling. Therefore, the power rating of the transformer should be taken as a decision variable and incorporated into the objective function of the planning model. It will be favourable to make a

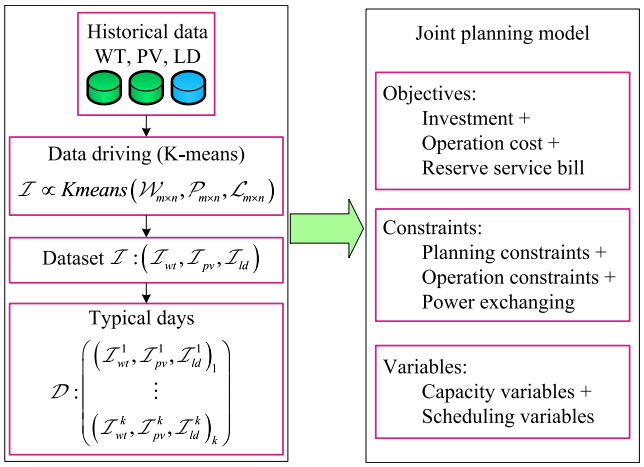

FIGURE 2. The two parts of the planning model.

TABLE 2. Definitions of symbols used in section III.

$\mathcal{W}_{m\times n}$, $\mathcal{P}_{m\times n}$, $\mathcal{L}_{m\times n}$	Historical data of WT, PV and load.
m, n	The number of days, number of time intervals.
$\mathcal{I}$	The data set of k classes.
$\mathcal{I}_{wt}^i$, $\mathcal{I}_{pv}^i$, $\mathcal{I}_{ld}^i$	The vector of WT, PV and load in i-th day.
$\mathcal{N}$	The set of day numbers of classes.
$\mathcal{N}_{ld}^i$	The number of days that belong to the i-th class of load.
$day^{i,\min}$	The day with the minimum values over time slots.
$day^{i,\max}$	The day with the maximum values over time slots.

trade-off between the capacity of RESs and the power rating of the transformer, to improve the economic outlook and viability of the planning scheme.

III. PSSMG PLANNING MODEL

In this paper, the planning model comprises two parts. The first part is a formulation of typical days based on a data-driven method and historical data, which is also regarded as preprocessing; the second part is a joint planning model, shown in Figure 2.

The purpose of the data preprocessing is to capture the underlying production and consumption patterns from the historical data. By doing so, most of the basic characteristics of the power uncertainties could be included by the typical days. Then, the typical days with most of the characteristics can be used to represent a full year time horizon. In the linear integrated planning model, the capacities sizing sub-problem and the energy management are integrated into one model, which is not calculated in a sequential way.

A. DATA-DRIVEN METHOD FOR COPING WITH UNCERTAINTIES IN PSSMG

In microgrids, RESs and loads are the main uncertainty sources. WT and PV are two kinds of most commonly used RESs. Their power outputs depending on the weather, which determines their stochastic intermittent nature. Generally, the penetration of RESs in PSSMG is high, so their uncertainties would cause significant random power fluctuation. On the other hand, loads in microgrids always depend on end-user patterns and vary with time, which may also result in the power fluctuation. All things considered, the uncertainties both on the power side and the load side would have a significant impact on the exchanging power and AEEA. For planning models, the uncertainty characteristics are obtained from the input data. Therefore, the ability to cope with the uncertainties of input data is important.

Due to the uncertainties, the power output of RESs and loads in each day varies. If we take every day as input the planning model may be more viable, but the scales of the variables would be prohibitive in a full year time horizon. Hence, in recent researches, probabilistic methods are often utilized to model and quantify the uncertainties, such as using Beta distribution function to model the uncertainty of PV and using Weibull distribution function to model the uncertainty of WT [22], [25]. Then, the Monte Carlo method is utilized to generate a large number of scenarios to imitate the real ones. However, it is hard to get the actual probabilistic distribution function and it will increase the computational burdens [18]. In order to tackle this problem, the typical day-types method is utilized to model a full year horizon in [18]. This may work in some way, but not all the outputs of RESs and loads in the same day-type are the same. A more effective identification method of typical days is needed. Hence, choosing typical days is not only important in reducing the number of variables, but also in handling the uncertainties in the planning model.

In this paper, a data-driven method based on the K-means algorithm is utilized to extract characteristics from one-year historical data and cluster historical data into different groups according to their similarities to obtain typical days. Shown in (2) - (6), historical data of WT, PV and load are classified into k classes. In each $\mathcal{I}_{wt}^i$, $\mathcal{I}_{pv}^i$ and $\mathcal{I}_{ld}^i$, the minimum value, the maximum value and the class center are included.

$$\mathcal{I} \propto Kmeans\,(\mathcal{W}_{m\times n}, \mathcal{P}_{m\times n}, \mathcal{L}_{m\times n}, k) \tag{2}$$

$$\mathcal{I} = \left\{ \begin{array}{c} \mathcal{I}^1 = \left(\mathcal{I}_{wt}^1, \mathcal{I}_{pv}^1, \mathcal{I}_{ld}^1\right) \\ \vdots \\ \mathcal{I}^k = \left(\mathcal{I}_{wt}^k, \mathcal{I}_{pv}^k, \mathcal{I}_{ld}^k\right) \end{array} \right\} \tag{3}$$

$$\mathcal{I}_{wt}^i = \left\{\mathcal{I}_{wt}^{i,\min}, \mathcal{I}_{wt}^{i,\max}, \mathcal{I}_{wt}^{i,\text{center}} \,|\forall i \in [1,k]\right\} \tag{4}$$

$$\mathcal{I}_{pv}^i = \left\{\mathcal{I}_{pv}^{i,\min}, \mathcal{I}_{pv}^{i,\max}, \mathcal{I}_{pv}^{i,\text{center}} \,|\forall i \in [1,k]\right\} \tag{5}$$

$$\mathcal{I}_{ld}^i = \left\{\mathcal{I}_{ld}^{i,\min}, \mathcal{I}_{ld}^{i,\max}, \mathcal{I}_{ld}^{i,\text{center}} \,|\forall i \in [1,k]\right\} \tag{6}$$

$$\mathcal{N} = \left\{\mathcal{N}_{ld}^1, \cdots, \mathcal{N}_{ld}^k\right\} \tag{7}$$

The process of obtaining typical days by the K-means algorithm is similar to the process of reducing and getting typical scenarios of stochastic optimization in handling the

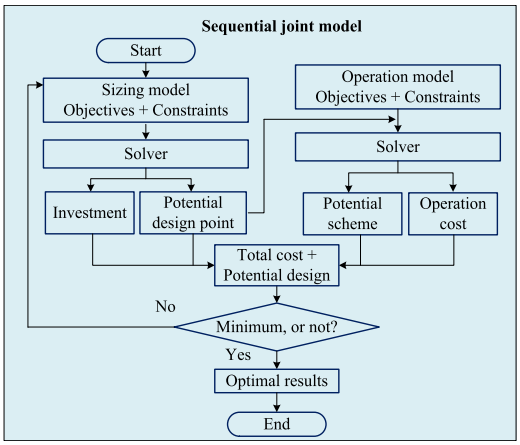

FIGURE 3. The typical flow chart of the sequential joint model.

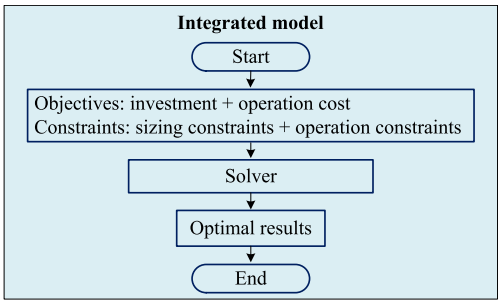

FIGURE 4. The flow chart of the proposed integrated model.

uncertainties. The difference is that the scenarios data set of stochastic optimization is generated according to a probability distribution function but the scenarios data set in this paper is obtained directly from historical data. By clustering, the typical days in this paper can represent the trend of variation of most scenarios.

Because load determines the capacities of generations, the day number of each load class is counted to represent the horizon of one full year. Based on the classified data classes, the data of typical days $\mathcal{D}$ are formulated by (8) - (11). In (11), $day^{i,\text{center}}$ is a typical day of the i-th class, which takes along the basic tendency information of the i-th class.

$$\mathcal{D} = \left\{ \begin{array}{cc} \left(day^{1,\min}, day^{1,\max}, day^{1,\text{center}}\right) \\ \vdots \qquad\qquad \vdots \\ \left(day^{k,\min}, day^{k,\max}, day^{k,\text{center}}\right) \end{array} \right\} \tag{8}$$

$$day^{i,\min} = \left(\mathcal{I}_{wt}^{i,\min}, \mathcal{I}_{pv}^{i,\min}, \mathcal{I}_{ld}^{i,\min}\right), \quad \forall i \in [1,k] \tag{9}$$

$$day^{i,\max} = \left(\mathcal{I}_{wt}^{i,\max}, \mathcal{I}_{pv}^{i,\max}, \mathcal{I}_{ld}^{i,\max}\right), \quad \forall i \in [1,k] \tag{10}$$

$$day^{i,\text{center}} = \left(\mathcal{I}_{wt}^{i,\text{center}}, \mathcal{I}_{pv}^{i,\text{center}}, \mathcal{I}_{ld}^{i,\text{center}}\right), \quad \forall i \in [1,k] \tag{11}$$

B. THE INTEGRATED PLANNING MODEL

Generally, a planning model could technically be categorized into three different types, namely, the independent planning model, the planning model sequentially combined with energy management and the integrated model. For the independent one, planning models are always carried out independently neglecting the operation of microgrids. However, the purpose of planning is to seek an optimal system configuration for operation. If the requirement of operation is not considered, the planning scheme maybe not result in optimal operation. For the second type, the operation requirement is combined with the planning model and solved in a sequential way. Although this combined model is much better than the independent one, the connection between the planning and the operation is not fully exploited. Each tested design point of sizing loop should be simulated in the management loop, which could lead to a prohibitive amount of CPU time [20].

Besides, many constraints calculated in the planning model should be recalculated in the operation model, such as system safety constraints. This repeated process may also increase the computational burden. In this paper, energy management is combined with the sizing model. The objective functions of the sizing and operation problem are constructed as a joint one, and their optimization variables are combined as one decision vector. The constraints of sizing and operation are integrated into one set, which only needs to be calculated once in the integrated model. The comparison between the sequential joint model and the proposed integrated model is shown in Figure 3 and Figure 4. The process of getting the optimal results in the sequential joint model is much more complex than that in the integrated model.

IV. INTEGRATED PLANNING PROBLEM FORMULATION

A. OBJECTIVE FUNCTION

The definitions of symbols in subsection A, section IV are shown in Table 3.

In this paper, the energy management for minimizing the operation cost is integrated into the planning model, so the objective function comprises both the investment and the operation costs. Because the reserve service bill charged by the utility operator would affect the sizing of the transformer at the PCC, it is also considered in the operational cost. The objective is to minimize the annual total cost, shown in (12)-(18).

$$\min f_c = M_{mg}^{inv} + M_{mg}^{opr} + M_{mg}^{rsb} \tag{12}$$

$$M_{mg}^{inv} = M_{total}^{inv}\left(r\left(1+r\right)^{\tau}\right) \Big/ \left(\left(1+r\right)^{\tau} - 1\right) \tag{13}$$

$$M_{total}^{inv} = \sum_{s} \gamma_s \pi_s^{inv} \mathbb{E}_s, \quad s \in \{S|pv, wt, de, es, tr\} \tag{14}$$

$$\gamma_s = cell\left(T/\tau_j\right), \quad s \in \{S|pv, wt, de, es, tr\} \tag{15}$$

$$M_{mg}^{opr} = M_{mg}^{ma} + \sum_{i=1}^{k} \mathcal{N}_{ld}^{i}\left(M_{de}^{opr,i} + M_{ex,b}^{opr,i} + M_{ex,s}^{opr,i}\right) \tag{16}$$

$$M_{mg}^{ma} = \sum_{s} \lambda_s \mathbb{E}_s, \quad s \in \{S|pv, wt, de, es, tr\} \tag{17}$$

TABLE 3. Definitions of symbols in subsection A.

M_{mg}^{inv}	The annualized investment cost.
$M_{total}^{inv}, M_{mg}^{opr}, M_{mg}^{ma}$	The total investment, operation, maintenance cost.
r	the bank interest.
τ	The the life expectancy of devices.
M_{de}^{opr}	The operation cost of DE.
$M_{ex,b}^{opr}$	The cost of purchasing electricity.
$M_{ex,s}^{opr}$	The profit of selling electricity.
M_{mg}^{rsb}	The reserve service bill.
$\pi_s^{inv}, \lambda_s, \mathbb{E}_s, \gamma_s$	The unit investment cost, unit maintenance cost, capacities, renewing times of different devices.
$\lambda_{de}^{i,j}$	The unit generation cost of DE.
$\lambda_{ex,b}^{i,j}$, $\lambda_{ex,s}^{i,j}$	The price of purchasing, selling electricity of the j-th time interval on the i-th typical day, respectively.
$p_{ex,b}^{i,j}, p_{ex,s}^{i,j}$	power flow of purchasing, selling electricity.
J	The number of time intervals in a day.
ΔT	The length of the time interval.
λ_{tr}^{u}	The price of reserve service in a month, \$/kWh.

$$\begin{cases} M_{de}^{opr,i} = \sum_{j=1}^{J} \lambda_{de}^{i,j} p_{de}^{i,j} \Delta \mathrm{T} \\ M_{ex,b}^{opr,i} = \sum_{j=1}^{J} \theta_{ex}^{i,j} \lambda_{ex,b}^{i,j} p_{ex,b}^{i,j} \Delta \mathrm{T} \\ M_{ex,s}^{opr,i} = \sum_{j=1}^{J} \left(1 - \theta_{ex}^{i,j}\right) \lambda_{ex,s}^{i,j} p_{ex,s}^{i,j} \Delta \mathrm{T} \end{cases} \tag{18}$$

$$M_{mg}^{rsb} = \sum_{u=1}^{12} \lambda_{tr}^{u} \mathbb{E}_{tr} \tag{19}$$

The annualized investment cost is calculated according to (13)-(15). The life expectancy is used to calculate the annualized investment cost in (13). If the lifetime of one device is shorter than the planning horizon, it needs to be replaced by a new one, the cost of a replacement should be included in the total investment cost. A coefficient is introduced to calculate the replacement times of devices by (15). In (15), T is the planning horizon of MG, function cell(·) means getting the nearest upper integer of a decimal. The total investment is calculated by (14). Take the i-th ($\forall i \in [1, k]$) typical day as an example, the operation cost includes the maintenance cost, the operation cost of DE and the operation cost of exchanging electricity, shwon in (16). In (18), $\theta_{ex}^{i,j}$ is a binary variable which indicates that the exchanging power is either purchasing electricity or selling electricity, $\theta_{ex}^{i,j} \in \{0, 1\}$. The reserve service bill is calculated by (19).

B. CONSTRAINTS

Take the i-th ($\forall i \in [1, k]$) typical day as an example. Power balance is the most important criteria. In PSSMGs, the load is supplied not only by PV, WD, DE and ESS but also by exchanging power (EXP). The power balance for a typical day is shown as (20).

$$\begin{bmatrix} \zeta_{pv}^{i,1} & \zeta_{wt}^{i,1} & & & \\ \vdots & \vdots & \mathbf{I}_{de} & \mathbf{I}_{es} & \mathbf{I}_{ex} \\ \zeta_{pv}^{i,J} & \zeta_{wt}^{i,J} & & & \end{bmatrix} \begin{bmatrix} \mathbb{E}_{pv} \\ \mathbb{E}_{wt} \\ \mathbf{P}_{de}^{i} \\ \mathbf{P}_{es}^{i} \\ \mathbf{P}_{ex}^{i} \end{bmatrix} = \begin{bmatrix} P_{ld}^{i,1} \\ \vdots \\ P_{ld}^{i,J} \end{bmatrix} \tag{20}$$

where, ζ_{pv}, ζ_{wt} represent the generation coefficient of PV and WT in a typical day, respectively; They are calculated from the historical data. $p_{ld}^{i,j}$ represents the load at j-th time interval in the i-th typical day; $\mathbf{I}_{de}$, $\mathbf{I}_{es}$, and $\mathbf{I}_{ex}$ represent the identity matrix of DE, ESS and EXP, respectively; $\mathbf{P}_{de}^{i}$, $\mathbf{P}_{es}^{i}$, and $\mathbf{P}_{ex}^{i}$ represent the power vector of DE, ESS and EXP in the i-th typical day, respectively, as shown in (21).

$$\begin{cases} \mathbf{P}_{de}^{i} = \left[p_{de}^{i,1}, p_{de}^{i,2}, \cdots, p_{de}^{i,J}\right]^{\mathrm{T}} \\ \mathbf{P}_{es}^{i} = \left[p_{es}^{i,1}, p_{es}^{i,2}, \cdots, p_{es}^{i,J}\right]^{\mathrm{T}} \\ \mathbf{P}_{ex}^{i} = \left[p_{ex}^{i,1}, p_{ex}^{i,2}, \cdots, p_{ex}^{i,J}\right]^{\mathrm{T}} \end{cases} \tag{21}$$

The power dispatch of the DE in each time interval of the i-th typical day should neither exceed its capacity nor fall below the minimum limit (22).

$$\begin{bmatrix} 0 \\ 0 \\ \vdots \\ 0 \end{bmatrix} \leq \begin{bmatrix} P_{de}^{i,1} \\ P_{de}^{i,2} \\ \vdots \\ P_{de}^{i,J} \end{bmatrix} \leq \begin{bmatrix} \mathbb{E}_{de} \\ \mathbb{E}_{de} \\ \vdots \\ \mathbb{E}_{de} \end{bmatrix} \tag{22}$$

In practice, $\mathbb{E}_{de}$ is not a constant, so (22) needs to be transformed into another form. The lower limit is shown as (23) and the upper limit is shown as (24).

$$\begin{bmatrix} -P_{de}^{i,1} \\ -P_{de}^{i,2} \\ \vdots \\ -P_{de}^{i,J-1} \\ -P_{de}^{i,J} \end{bmatrix} \leq \begin{bmatrix} 0 \\ 0 \\ \vdots \\ 0 \\ 0 \end{bmatrix} \tag{23}$$

$$\begin{bmatrix} P_{de}^{i,1} \\ P_{de}^{i,2} \\ \vdots \\ P_{de}^{i,J} \end{bmatrix} - \begin{bmatrix} \mathbb{E}_{de} \\ \mathbb{E}_{de} \\ \vdots \\ \mathbb{E}_{de} \end{bmatrix} \leq \begin{bmatrix} 0 \\ 0 \\ \vdots \\ 0 \end{bmatrix} \tag{24}$$

Then, the upper limit (24) is transformed to (25).

$$\begin{bmatrix} 1 & 0 & 0 & \cdots & -1 \\ 0 & 1 & 0 & \cdots & -1 \\ \vdots & & & \cdots & \vdots \\ 0 & 0 & \cdots & 1 & -1 \end{bmatrix} \begin{bmatrix} P_{de}^{i,1} \\ P_{de}^{i,2} \\ \vdots \\ P_{de}^{i,J} \\ \mathbb{E}_{de} \end{bmatrix} \leq \begin{bmatrix} 0 \\ 0 \\ \vdots \\ 0 \end{bmatrix} \tag{25}$$

Unlike the DE, ESS does not generate electric energy itself. It needs to store energy first and then discharge according to the requirement. So the initial energy state of ESS is also critical in the energy management of microgrids. But this is

often overlooked by specifying an arbitrary value. Furthermore, the energy state of ESS does not jump from one level to another suddenly. It needs to be accumulated with time and is tightly related to the current state and the power in the next time interval. Assume that the storage energy degradation and leakage effects are negligible [26], then, the relationship between energy states and charging or discharging power in each time interval is shown in (26).

$$\begin{cases} e^{i,1} = e^{i,0} - p_{es}^{i,1}\Delta T \\ e^{i,2} = e^{i,0} - p_{es}^{i,1}\Delta T - p_{es}^{i,2}\Delta T \\ \vdots \\ e^{i,J} = e^{i,0} - p_{es}^{i,1}\Delta T - p_{es}^{i,2}\Delta T - \cdots p_{es}^{i,J}\Delta T \end{cases} \tag{26}$$

where, $e^{i,0}$ indicates the initial energy state of ESS and $e^{i,j}$ indicates the energy state in j-th time interval of i-th typical day; ΔT is the length of the time interval.

In order to prolong the life expectancy of ESS, the energy state of ESS should not exceed the capacity or be lower than a certain value, usually $0.2\mathbb{E}_{es}$ for lithium-ion batteries. The constraints of ESS are shown as (27).

$$\begin{aligned} \begin{bmatrix} 0.2\mathbb{E}_{es} \\ 0.2\mathbb{E}_{es} \\ \vdots \\ 0.2\mathbb{E}_{es} \end{bmatrix} &\le \begin{bmatrix} e_0^i \\ e_0^i \\ \vdots \\ e_0^i \end{bmatrix} - \begin{bmatrix} 0 & 0 & \cdots & 0 \\ p_{es}^{i,1} & 0 & \cdots & 0 \\ \vdots & \vdots & \vdots & \vdots \\ p_{es}^{i,1} & p_{es}^{i,2} & \cdots & p_{es}^{i,J} \end{bmatrix} \begin{bmatrix} \Delta T \\ \Delta T \\ \vdots \\ \Delta T \end{bmatrix} \\ &\le \begin{bmatrix} \mathbb{E}_{es} \\ \mathbb{E}_{es} \\ \vdots \\ \mathbb{E}_{es} \end{bmatrix} \end{aligned} \tag{27}$$

Based on (27), the upper limit and lower limit of energy states are written as (28) and (29), respectively.

$$\begin{bmatrix} 1 & 0 & 0 & \cdots & -1 \\ 1 & -\Delta T & 0 & \cdots & -1 \\ \vdots & & & \cdots & \vdots \\ 1 & -\Delta T & \cdots & -\Delta T & -1 \end{bmatrix} \begin{bmatrix} e_0^i \\ p_{es}^{i,1} \\ \vdots \\ P_{es}^{i,J} \\ \mathbb{E}_{es} \end{bmatrix} \le \begin{bmatrix} 0 \\ 0 \\ \vdots \\ 0 \end{bmatrix} \tag{28}$$

$$\begin{bmatrix} -1 & 0 & 0 & \cdots & 0.2 \\ -1 & \Delta T & 0 & \cdots & 0.2 \\ \vdots & & & \cdots & \vdots \\ -1 & \Delta T & \cdots & \Delta T & 0.2 \end{bmatrix} \begin{bmatrix} e_0^i \\ p_{es}^{i,1} \\ \vdots \\ P_{es}^{i,J} \\ E_{es} \end{bmatrix} \le \begin{bmatrix} 0 \\ 0 \\ \vdots \\ 0 \end{bmatrix} \tag{29}$$

For ESS, the maximum charging power should not exceed the capacity, and the discharging power should be lower than the capacity. Hence, the upper limit and lower limit of charging power of ESS are written as (30) and (31), respectively. Wherein, the negative value indicates charging state and the positive value indicates discharging state.

$$\begin{bmatrix} 1 & 0 & 0 & \cdots & -1 \\ 0 & 1 & 0 & \cdots & -1 \\ \vdots & & & \cdots & \vdots \\ 0 & 0 & \cdots & 1 & -1 \end{bmatrix} \begin{bmatrix} p_{es}^{i,1} \\ p_{es}^{i,2} \\ \vdots \\ p_{es}^{i,J} \\ E_{es} \end{bmatrix} \le \begin{bmatrix} 0 \\ 0 \\ \vdots \\ 0 \end{bmatrix} \tag{30}$$

In order to keep the ESS in a sufficient energy state in each day, the energy state at the end of the last time interval is set as the same as the initial energy state (32).

$$\begin{bmatrix} -1 & 0 & 0 & \cdots & -0.5 \\ 0 & -1 & 0 & \cdots & -0.5 \\ \vdots & & & \cdots & \vdots \\ 0 & 0 & \cdots & -1 & -0.5 \end{bmatrix} \begin{bmatrix} p_{es}^{i,1} \\ p_{es}^{i,2} \\ \vdots \\ p_{es}^{i,J} \\ E_{es} \end{bmatrix} \le \begin{bmatrix} 0 \\ 0 \\ \vdots \\ 0 \end{bmatrix} \tag{31}$$

$$e^{i,J} = e^{i,0} \tag{32}$$

For a PSSMG, a portion of the electric power needs to be satisfied by the internal sources to ensure the exchanging power does not exceed the capacity of the transformer at the PCC (33). The total capacity of RESs should not be less than a certain value of the maximum load, such as 50% of the maximum load (34) and the annual exchanging electricity should not exceed a certain value as well, such as 50% of the annual electricity demand (35).

$$\begin{bmatrix} -\mathbb{E}_{tr} \\ -\mathbb{E}_{tr} \\ \vdots \\ -\mathbb{E}_{tr} \end{bmatrix} \le \begin{bmatrix} p_{ex}^{i,1} \\ p_{ex}^{i,2} \\ \vdots \\ p_{ex}^{i,J} \end{bmatrix} \le \begin{bmatrix} \mathbb{E}_{tr} \\ \mathbb{E}_{tr} \\ \vdots \\ \mathbb{E}_{tr} \end{bmatrix} \tag{33}$$

$$\mathbb{E}_{pv} + \mathbb{E}_{wd} \ge \gamma_{res} \max\left(p_{ld}\right) \tag{34}$$

$$\sum_{i=1}^{k} \left(\mathcal{N}_{ld}^{i} \sum_{j=1}^{J} \left| p_{ex}^{i,j} \right| \right) \le \gamma_{ex} \sum_{i=1}^{k} \mathcal{N}_{ld}^{i} \sum_{j=1}^{J} p_{ld}^{i,j} \tag{35}$$

where, p_{ex} is the exchanging power; γ_{ex}, γ_{res} represent the percentage of exchanging electricity and penetration of RESs, respectively.

Due to the uncertainties of RESs, some extreme situations may happen. So, the capacities of dispatchable DGs and TR need to be sufficient to guarantee the power supply. The combined capacity of DE, ESS and TR should be larger than the maximum load (36).

$$\mathbb{E}_{de} + \mathbb{E}_{ess} + \mathbb{E}_{tr} \ge \max\left(p_{ld}\right) \tag{36}$$

1) MODEL LINEARIZATION

As shown in (18), because the exchanging power is bidirectional and the purchasing price and selling price are different, a binary variable $\theta_{ex}^{i,j}$ is introduced in the integrated planning model to specify the direction of exchanging power. Besides, the constraint of exchanging power (34) contains an absolute operator. These make the planning model non-linear, which belongs to the class of NP-hard problem and cannot be solved within polynomial time. In this paper, a linearization method

based on our previous work [27] is introduced to transfer the bi-linear objective into a linear one. In addition, a method dealing with the non-linear constraint with an absolute operator is proposed.

Recall (16) and (18), let $M_{ex}^{opr,i}$ indicate the operation cost of exchanging power in a typical day, $p_{ex}^{i,j}$ indicate the exchanging power in a typical day and $\lambda_{ex}^{i,j}$ indicate the exchanging electricity price in a typical day. Then, the operation cost of the microgrid is rewritten as (37) - (38).

$$\begin{cases} M_{mg}^{opr} = M_{mg}^{ma} + \sum_{i=1}^{k} \mathcal{N}_{ld}^{i} \left(M_{mt}^{opr,i} + M_{ex}^{opr,i} \right) \\ M_{ex}^{opr,i} = \sum_{j=1}^{J} \lambda_{ex}^{i,j} p_{ex}^{i,j} \Delta \mathrm{T} \end{cases} \tag{37}$$

$$\begin{cases} \lambda_{ex}^{i,j} = \begin{cases} \lambda_{ex,b}^{i,j}, & if\ p_{ex}^{i,j} \geq 0 \\ \lambda_{ex,s}^{i,j}, & if\ p_{ex}^{i,j} < 0 \end{cases} \\ p_{ex}^{i,j} = p_{ld}^{i,j} - p_{de}^{i,j} - p_{pv}^{i,j} - p_{wt}^{i,j} - p_{es}^{i,j} \end{cases} \tag{38}$$

Because (38) is a piecewise function, the optimization problem cannot be solved by existing optimization tools directly. Therefore, (37) with (38) is transformed to (39) and then to (40) and (41) according to [27], which are equivalent linear functions. To keep the readability of the paper, the detailed transformation process is not presented in the main text but presented in Appendix A, which is at the end of the paper.

$$\begin{cases} M_{mg}^{opr} = M_{mg}^{ma} + \sum_{i=1}^{k} \mathcal{N}_{ld}^{i} \left(M_{de}^{opr,i} + M_{ex}^{opr,i} \right) \\ M_{ex}^{opr,i} = \sum_{j=1}^{J} \frac{\Delta \mathrm{T}}{2} \left(\left(\lambda_{ex,b}^{i,j} - \lambda_{ex,s}^{i,j} \right) \left| p_{ex}^{i,j} \right| + \left(\lambda_{ex,b}^{i,j} + \lambda_{ex,s}^{i,j} \right) p_{ex}^{i,j} \right) \end{cases} \tag{39}$$

$$\begin{cases} M_{mg}^{opr} = M_{mg}^{ma} + \sum_{i=1}^{k} \mathcal{N}_{ld}^{i} \left(M_{de}^{opr,i} + M_{ex}^{opr,i} \right) \\ M_{ex}^{opr,i} = \sum_{j=1}^{J} \frac{\Delta \mathrm{T}}{2} \left(\left(\lambda_{ex,b}^{i,j} - \lambda_{ex,s}^{i,j} \right) \left(g_b^j + g_s^j \right) + \left(\lambda_{ex,b}^{i,j} + \lambda_{ex,s}^{i,j} \right) p_{ex}^{i,j} \right) \end{cases} \tag{40}$$

$$\begin{cases} p_{ex}^{i,j} + g_b^j - g_s^j = 0 \\ g_b^j \geq 0, \quad g_s^j \geq 0 \end{cases}, \forall j \in J \tag{41}$$

where, g_b^j and g_s^j are auxiliary variables.

By linearizing the objective function, $p_{ex,b}^{i,j}$ and $p_{ex,s}^{i,j}$ are unified described by the exchanging power $p_{ex}^{i,j}$. So, the constraint of exchanging power in (33) is further transformed as (42) - (43).

$$\begin{bmatrix} 1 & 0 & 0 & \cdots & -1 \\ 0 & 1 & 0 & \cdots & -1 \\ \vdots & & & \cdots & \vdots \\ 0 & 0 & \cdots & 1 & -1 \end{bmatrix} \begin{bmatrix} p_{ex}^{i,1} \\ p_{ex}^{i,2} \\ \vdots \\ p_{ex}^{i,J} \\ \mathbb{E}_{tr} \end{bmatrix} \leq \begin{bmatrix} 0 \\ 0 \\ \vdots \\ 0 \end{bmatrix} \tag{42}$$

$$\begin{bmatrix} -1 & 0 & 0 & \cdots & -1 \\ 0 & -1 & 0 & \cdots & -1 \\ \vdots & & & \cdots & \vdots \\ 0 & 0 & \cdots & -1 & -1 \end{bmatrix} \begin{bmatrix} p_{ex}^{i,1} \\ p_{ex}^{i,2} \\ \vdots \\ p_{ex}^{i,J} \\ \mathbb{E}_{tr} \end{bmatrix} \leq \begin{bmatrix} 0 \\ 0 \\ \vdots \\ 0 \end{bmatrix} \tag{43}$$

Regarding the constraint (35), the absolute operator needs to be further transferred. Let $y^{i,j}$ indicate the absolute value of exchanging power, shown as (44).

$$y^{i,j} = \left| p_{ex}^{i,j} \right| \tag{44}$$

Then, from (35) we have (45).

$$\sum_{i=1}^{\mathcal{N}} \left(\mathcal{N}_{ld}^{i} \sum_{j=1}^{J} y^{i,j} \right) \leq \gamma_{ex} \sum_{i=1}^{\mathcal{N}} \mathcal{N}_{ld}^{i} \sum_{j=1}^{J} p_{ld}^{i,j}, \quad y^{i,j} \geq 0 \tag{45}$$

Let $\mathbf{x}$ indicate the variables vector of the current model, $f(\mathbf{x})$ indicate the original linear objective function and $g(\mathbf{y})$ indicate a linear function of $y^{i,j}$. Then, we can formulate a new objective function (46) and corresponding constraints (47).

$$\min F = f(\mathbf{x}) + g(\mathbf{y}) \tag{46}$$

$$\begin{cases} g(\mathbf{y}) = \mathbf{a}\mathbf{y}^{\mathrm{T}}, \quad \mathbf{a} \to 0 \\ \mathbf{x} \in h(\mathbf{x}) \\ y^{i,j} \geq 0, \qquad y^{i,j} \geq p_{ex}^{i,j}, \quad y^{i,j} \geq -p_{ex}^{i,j} \end{cases} \tag{47}$$

where, $\mathbf{a}$ is the coefficient vector; $\mathbf{y}^{\mathrm{T}}$ is the column vector of $y^{i,j}$; $h(\mathbf{x})$ is the set of constraints formulated in the original problem (20) - (36) and (42) - (43).

Next, we are going to prove the equivalent condition between the original objective and the new one. In (46), $f(\mathbf{x})$ and $g(\mathbf{y})$ are both linear function. So F will obtain its minimum value only if $f(\mathbf{x})$ and $g(\mathbf{y})$ are both at their minimum, $f(\mathbf{x}*)$ and $g(\mathbf{y}^*)$, respectively. $\mathbf{x}^*$ is the optimal solution of the original problem. Because $g(\mathbf{y})$ is a linear function, $g(\mathbf{y}^*)$ will be obtained at the lower bound of $\mathbf{y}^{\mathrm{T}}$, namely (48).

$$g\left(\mathbf{y}^*\right) = \sum_{j=1}^{J} a^{i,j} \left| p_{ex}^{i,j} \right|, \quad \mathbf{y}^* = \left[\left| p_{ex}^{i,1} \right|, \cdots, \left| p_{ex}^{i,J} \right| \right] \tag{48}$$

So, when the new problem F gets its minimum value, (45) is equivalent to (35). However, in order not to impact the minimum value of the objective of the original problem, the coefficient vector $\mathbf{a}$ needs to be further determined. The minimum value of F, shown in (49), is not equal to the original problem.

$$F^* = f(\mathbf{x}^*) + g\left(\mathbf{y}^*\right) \tag{49}$$

If (49) equals to the original one only when (50) is held, namely, $g(\mathbf{y}^*)$ is small enough.

$$g\left(\mathbf{y}^*\right) \to 0 \tag{50}$$

Then, according to (48), $a^{i,j}$ needs to be sufficiently small, as in (51).

$$a^{i,j} \to 0, \quad \forall i \in [1, \mathcal{N}],\ j \in [1, J] \tag{51}$$

2) MODEL SCALE-UP

At present, all the constraints are described using a typical day. In this paper, the k classes of typical days are utilized to scale up the model to a full year horizon by the number of typical days in set $\mathcal{N}$.

The overall integrated planning model after linearization and scaling up is shown as (52) - (60).

$$\min\ F = f\left(\mathbf{x}\right) + g\left(\mathbf{y}\right) \tag{52}$$

$$f\left(\mathbf{x}\right) = M_{mg}^{inv} + M_{mg}^{opr} + M_{mg}^{rsb}$$

$$g\left(\mathbf{y}\right) = \sum_{i=1}^{k} \mathcal{N}_{ld}^{i} \sum_{j=1}^{J} a^{i,j} y^{i,j} \tag{53}$$

$$M_{mg}^{inv} = M_{total}^{inv}\left(r\left(1+r\right)^{\tau}\right) \Big/ \left(\left(1+r\right)^{\tau} - 1\right) \tag{54}$$

$$M_{total}^{inv} = \left(\pi_{pv}^{inv}\mathbb{E}_{pv} + \pi_{wt}^{inv}\mathbb{E}_{wt} + \pi_{de}^{inv}\mathbb{E}_{de} + \pi_{es}^{inv}\mathbb{E}_{es} + \pi_{tr}^{inv}\mathbb{E}_{tr}\right) \tag{55}$$

$$M_{mg}^{opr} = \sum_{i=1}^{k} \mathcal{N}_{ld}^{i}\left(M_{de}^{opr,i} + M_{ex}^{opr,i}\right) \tag{56}$$

$$M_{ex}^{opr,i} = \sum_{j=1}^{J} \frac{\Delta \mathrm{T}}{2}\left(\left(\lambda_{ex,b}^{i,j} - \lambda_{ex,s}^{i,j}\right)\left(g_b^j + g_s^j\right) + \left(\lambda_{ex,b}^{i,j} + \lambda_{ex,s}^{i,j}\right)p_{ex}^{i,j}\right)$$

$$M_{mg}^{rsb} = \sum_{u=1}^{12} \lambda_{tr}^{u}\mathbb{E}_{tr} \tag{57}$$

$$\mathbf{x} \in h\left(\mathbf{x}\right) \tag{58}$$

$$\begin{bmatrix} -1 & 0 & \cdots & 0 & -1 & 0 & \cdots & 0 \\ 0 & -1 & & 0 & 0 & -1 & & 0 \\ \vdots & & & \vdots & \vdots & & & \vdots \\ 0 & 0 & \cdots & -1 & 0 & 0 & \cdots & -1 \end{bmatrix} \begin{bmatrix} y^{i,1} \\ \vdots \\ y^{i,J} \\ p_{ex}^{i,1} \\ \vdots \\ p_{ex}^{i,J} \end{bmatrix} \leq \begin{bmatrix} 0 \\ \vdots \\ 0 \\ 0 \\ \vdots \\ 0 \end{bmatrix} \tag{59}$$

$$\begin{bmatrix} -1 & 0 & \cdots & 0 & 1 & 0 & \cdots & 0 \\ 0 & -1 & & 0 & 0 & 1 & & 0 \\ \vdots & & & \vdots & \vdots & & & \vdots \\ 0 & 0 & \cdots & -1 & 0 & 0 & \cdots & 1 \end{bmatrix} \begin{bmatrix} y^{i,1} \\ \vdots \\ y^{i,J} \\ p_{ex}^{i,1} \\ \vdots \\ p_{ex}^{i,J} \end{bmatrix} \leq \begin{bmatrix} 0 \\ \vdots \\ 0 \\ 0 \\ \vdots \\ 0 \end{bmatrix} \tag{60}$$

All the decision variable vectors after being scaled up is shown as (61) - (68).

$$\mathbf{x} = \left[\mathbb{E}_{wd}, \mathbb{E}_{pv}, \mathbb{E}_{mt}, \mathbb{E}_{es}, \mathbb{E}_{tr}, e_0, \mathbf{P}_{day}^{1}, \cdots, \mathbf{P}_{day}^{k}\right]^{\mathrm{T}} \tag{61}$$

$$\mathbf{P}_{day}^{i} = \left[\mathbf{p}_{de}^{i}, \mathbf{p}_{es}^{i}, \mathbf{p}_{ex}^{i}, \mathbf{G}_{b}^{i}, \mathbf{G}_{s}^{i}, \mathbf{Y}^{i}\right], \quad i \in [1, k] \tag{62}$$

$$\mathbf{P}_{de}^{i} = \left[p_{de}^{i,1}, \cdots, p_{de}^{i,J}\right], \quad i \in [1, k] \tag{63}$$

$$\mathbf{P}_{es}^{i} = \left[p_{es}^{i,1}, \cdots, p_{es}^{i,J}\right], \quad i \in [1, k] \tag{64}$$

$$\mathbf{P}_{ex}^{i} = \left[p_{ex}^{i,1}, \cdots, p_{ex}^{i,J}\right], \quad i \in [1, k] \tag{65}$$

$$\mathbf{G}_{b}^{i} = \left[g_{b}^{i,1}, \cdots, g_{b}^{i,J}\right], \quad i \in [1, k] \tag{66}$$

$$\mathbf{G}_{s}^{i} = \left[g_{s}^{i,1}, \cdots, g_{s}^{i,J}\right], \quad i \in [1, k] \tag{67}$$

$$\mathbf{Y}_{s}^{i} = \left[y^{i,1}, \cdots, y^{i,J}\right], \quad i \in [1, k] \tag{68}$$

where $\mathbf{P}_{day}^{i}$is the dispatch variable vector on the i-th typical day; $\mathbf{P}_{de}^{i}$ is the dispatch power variable vector of DE on the i-th typical day; $\mathbf{P}_{es}^{i}$ is the dispatch power variable vector of ESS on the i-th typical day; $\mathbf{P}_{ex}^{i}$ is the dispatch power variable vector of ESS on the i-th typical day; $\mathbf{G}_{b}^{i}$, $\mathbf{G}_{s}^{i}$ and $\mathbf{Y}_{s}^{i}$ are the three auxiliary variable vectors.

So far, all the objectives and constraints are modeled as a set of linear equations and are scaled up to a full year horizon. So the integrated planning model can be solved by a linear program method.

V. NUMERICAL STUDY

A. SIMULATION PARAMETERS

In this section, a PSSMG with WT, PV, DE and ESS is taken as an example. The time horizon for planning is one year with a time interval of 1 hour. The key parameters of DGs, ESS and TR are shown in table 4, 5, 6, respectively [17], [28]. The planning horizon is 15 years. The designed life expectancies of all the equipment are assumed to be 15 years, except the ESS is 10 years. Because the lifetime of ESS is shorter than the planning horizon, it has to be replaced at the end of life expectancy and the replacement cost is also included in this model. The time of use (TOU) price of buying electricity and

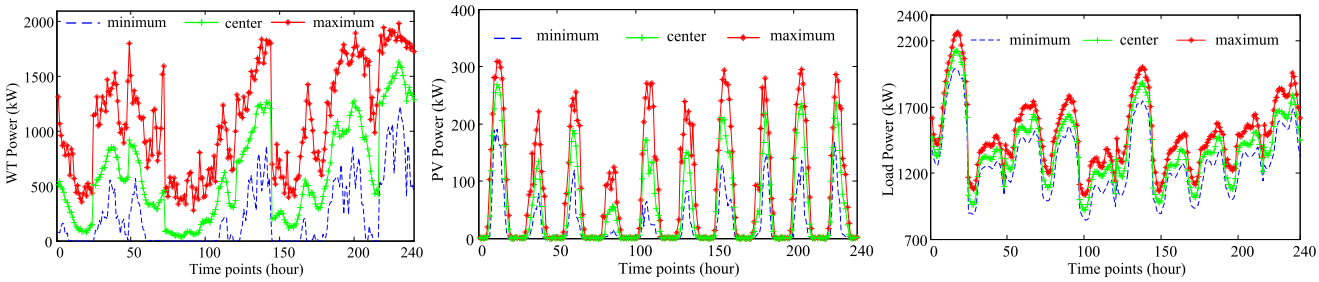

FIGURE 5. The minimum values, maximum values and centers of ten classes of WT, PV and load (WT capacity 2.3MW, PV capacity 350 kW).

TABLE 4. Parameters of candidate DGs.

Label	Capital cost ($/kW)	O & M cost ($/kW/year)	Feul cost ($/kWh)	Life time
WT	1600	40	/	15
PV	1400	35	/	15
DE	210	18	0.1886	15

TABLE 5. Parameters of energy storage system.

Label	Capital cost ($/kWh)	O & M cost ($/kW/year)	Life time
ESS	450	5	10

TABLE 6. Parameters of transformer.

Label	Capital cost ($/kWh)	Reserve cost ($/kW/month)	Life time
TR	450	2.5	15

TABLE 7. Price of buying electricity.

Time	Price ($/kWh)	Time	Price ($/kWh)
1:00-6:00	0.0554	18:00-20:00	0.1919
7:00-9:00	0.1218	21:00-22:00	0.1218
10:00-14:00	0.1919	23:00-24:00	0.0554
15:00-17:00	0.1218		

TABLE 8. Price of selling electricity.

Time	Price ($/kWh)	Time	Price ($/kWh)
1:00-6:00	0.0554	18:00-20:00	0.0620
7:00-9:00	0.0620	21:00-22:00	0.0620
10:00-14:00	0.0620	23:00-24:00	0.0554
15:00-17:00	0.0620		

selling electricity are shown in table 7 and table 8, respectively. $a^{i,j} = 10^{-10}$.

In this section, the historical data of WT, PV and load is classified into ten typical classes. The maximum value, the minimum value and the centroid value of each class are utilized to form the generation of three different scenarios, shown in Figure 5. The peak load is 2,267 kW. Considering some real limitation, such as land area, the upper bounds of WT and PV are set as 80% of the maximum load.

In order to verify the validity of the proposed model, four scenarios are conducted in this section.

Scenario 1: the maximum value of WT, PV and load in ten typical days are used as the input data for the proposed model; Scenario 2: the minimum value of WT, PV and load in ten typical days are used as the input data for the proposed model;

Scenario 3: the centroid value of WT, PV and load in ten typical days are used as the input data for the proposed model.

Scenario 4: typical day selection method used in [6], namely, one typical day in each season is used as input data for the proposed model. Because typical days cannot represent all the information of a full year, after getting the results, further evaluation for a full year operation is carried out to verify the viability of the planning scheme obtained by each scenario. The scheme viability index (SVI), defined as the ratio between the estimated total cost by the planning model and actual total cost from the evaluation is used to evaluate the reliability of the planning scheme.

B. RESULTS ANALYSIS

The four comparison simulation results are shown in Table 9 and Fig. 6, and the evaluation results are shown in Table 10.

The planning input data in scenario 1 is the maximum values of WT and PV assuming a high efficiency of RESs generation, which implies that it is very economical to supply the load demand using RESs. Therefore, the capacity of RESs in scenario 1 is the largest and many batteries are installed and supposed to store the surplus power from RESs. If the output of RESs in a full year is similar to the input data, which implies a high efficiency as shown in Fig. 6 (a), the overall cost is lower because of selling a lot of electricity to the distribution network. However, in scenario 1, the generation efficiency of RESs in most of the days in one full year cannot reach that high level, and thus causes a high actual operation and maintenance (O & M) cost. The actual O & M cost is

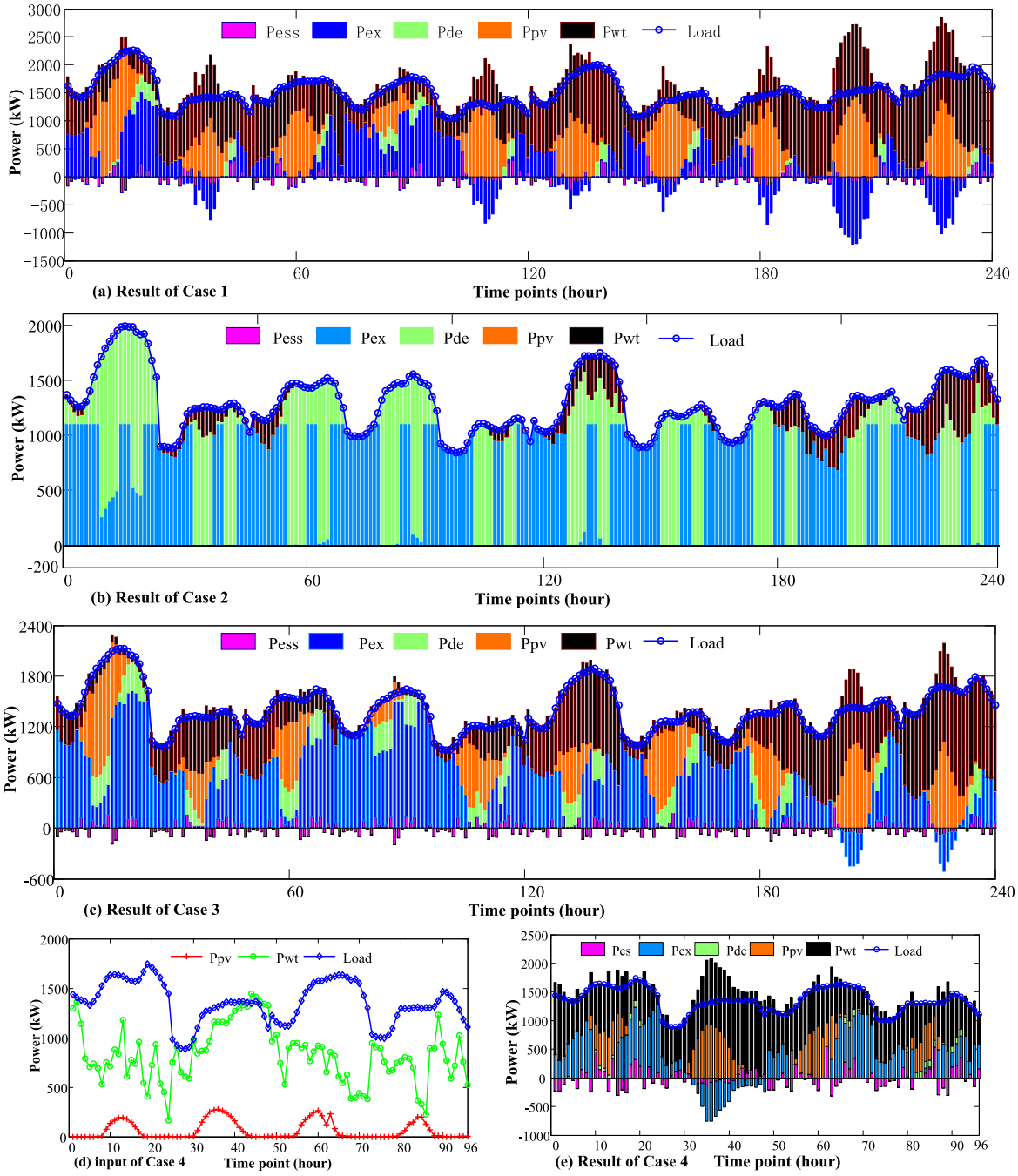

FIGURE 6. Simulation results of four comparison scenarios.

0.9884 million $ which is almost 2.52 times than the estimated O & M cost, shown in Table 10. Finally, the planning scheme in scenario 1 results in a higher total cost. Comparing Table 9 with Table 10, the actual total cost is much higher than the estimated total cost, which results in lower scheme viability, 62.83%. Due to the uncertainty of RESs, the actual exchanging power is 52.72%, which is slightly above the limit. So the planning scheme obtained in scenario 1 is not only unreliable but also not economical.

In scenario 2, due to the lowest efficiency of the input RESs generation data, the RESs with lowest capacities are installed to meet the minimum capacity limitation, 50% of the maximum load. Due to the limitation of the exchanging electricity, DEs with large capacities are installed to supply most of the load demand. So, most of the power is supplied by the internal DEs and the distribution network, see Fig. 6 (b). This would lead to a high O & M cost and total cost. Actually, the total cost in scenario 2 is the highest, but the

TABLE 9. Price of selling electricity.

	Scenario 1	Scenario 2	Scenario 3	Scenario 4
WT (kW)	1814	1134	1814	1814
PV (kW)	1509	0	1476	1188
DE (kW)	318	1459	349	115
ESS (kWh)	678	0	418	967
TR (kW)	1271	1105	1499	1186
Capital cost (m$/year)	0.5642	0.2194	0.5425	0.5421
Estimated O &M cost (m$/year)	0.3972	1.3631	0.8094	0.4416
Reserve cost(m$/year)	0.0381	0.0332	0.0450	0.0356
Estimated total cost (m$/year)	0.9995	1.6157	1.3969	1.0193

TABLE 10. Evaluation results of four scenarios.

	Scenario 1	Scenario 2	Scenario 3	Scenario 4
Capital cost (m$/year)	0.5642	0.2194	0.5425	0.5421
Actual O &M cost (m$/year)	0.9884	1.4064	0.9640	1.0647
Reserve cost(m$/year)	0.0381	0.0332	0.0450	0.0356
Actual total cost (m$/year)	1.5907	1.6590	1.5515	1.6424
Actual exchanging power (%)	52.72%	49.02%	50.36%	57.16%
Scheme viability index (%)	62.83%	97.39%	90.04%	62.06%

exchanging power is 49.02% which is within the limitation and the scheme viability is 97.39%. This is because that (1) the actual power of RESs in one full year is larger the typical input date (lowest output efficiency of RESs) in scenario 2; (2) the capacity of RESs is lowest and less than the capacity of DE and load, all the power generated by RESs could be consumed within the microgrid and the uncertainty could be well regulated by DEs.

In scenario 3, because the input data of RESs in typical days are selected by the K-means method, the data could carry most of the actual situations and is much similar to the actual characteristics in one full year. Thus the estimated total cost is much closer to the actual total cost and the scheme viability index is much larger than that in scenario 1 and scenario 4. But the actual exchanging power is 50.36% which is slightly over the limitation due to the uncertainty of RESs.

In scenario 4, the actual total cost of the planning scheme is much higher than that in scenario 1 and scenario 3, because the four typical days selected by experiences from each season are not representative enough for the characteristics in one full year. Besides, the scheme viability index is the lowest and the actual exchanging power is much higher than the limitation.

From the results of the four comparison cases, it can be concluded that:

(1) Regarding the scheme viability index and the exchanging electricity rate, scenario 2 may be the best option. But its total cost is the highest, which is unacceptable. Besides, the planning scheme is too extreme.
(2) Although the scheme viability index and the exchanging electricity rate in scenario 3 are not better than that in scenario 2, its total cost is the most economical and the capacity structure is much better than that in scenario 2. Besides, the scheme viability index is acceptable and the exchanging electricity rate is very close to the limit. The limit is slightly violated, but it could easily be solved in real operation.
(3) It is important for the planning model to select a suitable set of input data that include enough characteristics of one full year. Otherwise, the scheme obtained by the planning model may not be reliable.
(4) Due to the uncertainty of RESs, the planning scheme may not ensure that the exchanging power does not exceed the limit exactly. It also needs to optimize the operation of MG according to the actual situation.

C. CALCULATION EFFICIENCY ANALYSIS

The complicity and calculation burden is another important factor. In this paper, the complicity is reduced and the calculation efficiency is improved in three aspects.

(1) In order to reduce the computational burden and improve the efficiency of the proposed integrated planning model, a data-driven method based on the K-means algorithm is utilized to choose a typical set of input data to reduce the number of variables in one full year horizon. The number of optimization variables in the proposed model is 1446, which is only 2.75% of the number of variables in the unsimplified problem. By using the K-means algorithm to obtain typical days is much simpler than the process of scenarios generating and reducing in stochastic planning. It is no

TABLE 11. Planning scheme with different EERs.

	EER⩾0.5	EER =0.4	EER=0.3	EER=0.2	EER=0.15	EER=0.1	EER=0
WT (kW)	1814	1814	1814	1814	1814	1814	1814
PV (kW)	1476	1529	1480	1480	1108	1108	1088
DE (kW)	349	610	1281	1281	1579	1814	1814
ESS (kWh)	418	412	0	0	0	0	710
TR (kW)	1499	1245	986	986	688	453	0
Actual total cost (m$/year)	1.5515	1.5582	1.5911	1.5911	1.7024	1.8126	2.0783

need to get the distribution function and then generate scenarios by Monte Carlo algorithm.

(2) The planning problem is modeled in a linear form so that the model could be easily solved in polynomial time. Otherwise, the computational burden would increase exponentially as the number of variables grows.

(3) The sizing sub-problem and operation sub-problem are combined as one model, and there is no need to calculate sequentially, whereas a two-stage model needs to calculate the sizing problem first, and then calculate the operation problem sequentially. The most important factor is that it may take a prohibitive amount of CPU time to simulate over a long period (such as a full year) of time for every tested design point generated by the sizing loop [20].

The proposed integrated model is solved by a computer with i7-3632QM CPU and 4 GB memory. The time of solving the proposed integrated planning model is about 0.815 seconds. However, the total time of solving two-stage model is composed of the time of solving sizing loop and the time of evaluating the results from sizing loop. The time of evaluating once with 365 days is about 8.184 seconds. So it may take many times longer than 8.184 seconds to get the optimal value in the two-stage model, which would take much longer than the proposed model.

D. SENSITIVITY ANALYSIS

The limitation of exchanging electricity and the number of classes are two of the most important elements affecting the planning scheme. In this part, the impact of electricity exchanging rate (EER) and the number of classes on the planning scheme are analyzed, shown in Fig. 7, Fig. 8 and Table 11.

In Fig. 7, the annual total cost would increase with the decrease in electricity exchanging rate in a certain range, EER $\in$ [0, 0.5]. This is because when the electricity exchanging rate decreases, more load demand has to be supplied by internal generations. Thus, the PSSMG needs to increase the capacity of DE, which would result in a high operation cost. But as the EER continue increasing from 0.5 to 1, the sizing scheme and the total cost would not change. This is because

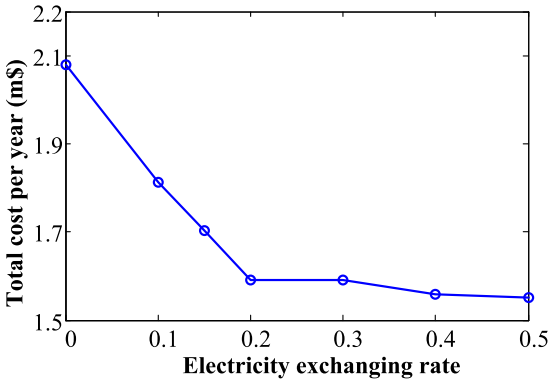

FIGURE 7. Total annual cost VS electricity exchanging rate.

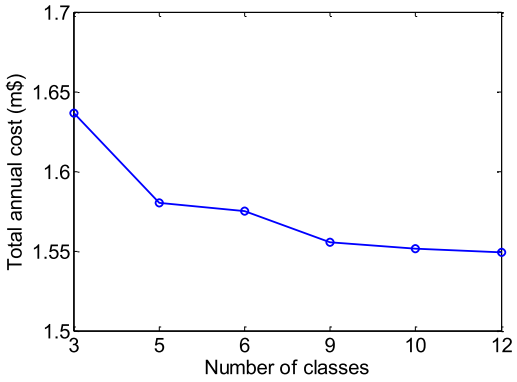

FIGURE 8. Total annual cost VS number of classes.

the sizing scheme with EER = 0.5 is also the optimal scheme for an on-grid MG without any electricity exchanging limit.

In Fig. 8, the annual total cost would decrease with the number of classes increases. But the decrease rate tends to be smaller when the number of classes is larger than 10.

VI. CONCLUSION

In order to solve the planning problem for microgrids with a limited AEEA, a planning method has been proposed in this paper. The sizing problem and operation problem are jointly considered in one model with a linear formulation. Typical days identified by a data-driven method based on the K-means algorithm are utilized as an input to reduce the number of optimization variables substantially.

Compared with a two-stage model, no interacting loop is needed, which makes the proposed integrated model to be more concise. Thus, the computational burden could be reduced dramatically. Besides, the proposed integrated planning model is built in a linear way, so it could be solved in polynomial time.

In addition, since the typical days identified by the data-driven method based on the K-means algorithm are representative of the historical data of one full year, the planning scheme is much more reliable.

Although the limitation of AEEA is considered in the planning model, the actual operation situation may be different from the typical days. This may result in the AEEA exceeding the limit. Hence, real operation needs to be adjusted to respect the limitation.

APPENDIX

This appendix proves that (37) with the piecewise function (38) is equivalent to (39), and then equivalent to linear functions (40) and (41). (37)-(41) have been presented as follows again for convenience.

$$\begin{cases} M_{mg}^{opr} = M_{mg}^{ma} + \sum_{i=1}^{k} \mathcal{N}_{ld}^{i} \left(M_{mt}^{opr,i} + M_{ex}^{opr,i} \right) \\ M_{ex}^{opr,i} = \sum_{j=1}^{J} \lambda_{ex}^{i,j} p_{ex}^{i,j} \Delta \mathrm{T}. \end{cases} \tag{37}$$

$$\begin{cases} \lambda_{ex}^{i,j} = \begin{cases} \lambda_{ex,b}^{i,j}, & if\ p_{ex}^{i,j} \geq 0 \\ \lambda_{ex,s}^{i,j}, & if\ p_{ex}^{i,j} < 0 \end{cases} \\ p_{ex}^{i,j} = p_{ld}^{i,j} - p_{de}^{i,j} - p_{pv}^{i,j} - p_{wt}^{i,j} - p_{es}^{i,j}. \end{cases} \tag{38}$$

$$\begin{cases} M_{mg}^{opr} = M_{mg}^{ma} + \sum_{i=1}^{k} \mathcal{N}_{ld}^{i} \left(M_{de}^{opr,i} + M_{ex}^{opr,i} \right) \\ M_{ex}^{opr,i} = \sum_{j=1}^{J} \frac{\Delta \mathrm{T}}{2} \left(\left(\lambda_{ex,b}^{i,j} - \lambda_{ex,s}^{i,j} \right) \left| p_{ex}^{i,j} \right| \right. \\ \qquad \left. + \left(\lambda_{ex,b}^{i,j} + \lambda_{ex,s}^{i,j} \right) p_{ex}^{i,j} \right). \end{cases} \tag{39}$$

$$\begin{cases} M_{mg}^{opr} = M_{mg}^{ma} + \sum_{i=1}^{k} \mathcal{N}_{ld}^{i} \left(M_{de}^{opr,i} + M_{ex}^{opr,i} \right) \\ M_{ex}^{opr,i} = \sum_{j=1}^{J} \frac{\Delta \mathrm{T}}{2} \left(\left(\lambda_{ex,b}^{i,j} - \lambda_{ex,s}^{i,j} \right) \left(g_b^j + g_s^j \right) \right. \\ \qquad \left. + \left(\lambda_{ex,b}^{i,j} + \lambda_{ex,s}^{i,j} \right) p_{ex}^{i,j} \right). \end{cases} \tag{40}$$

$$\begin{cases} p_{ex}^{i,j} + g_b^j - g_s^j = 0 \\ g_b^j \geq 0, \quad g_s^j \geq 0 \end{cases}, \forall j \in J \tag{41}$$

Actually, similar conclusions have been drawn in Appendix B of [27], but the detailed proof in the context of this paper is still presented as follows.

A. PROOF OF (39) BEING EQUIVALENT TO (37) WITH (38)

In this section, it will be proved that (39) is equivalent to (37) with (38). The proof includes two parts.

For the first part of the proof, when $p_{ex}^{i,j} \geq 0$, based on (37) and 38, there is

$$M_{ex}^{opr,i} = \sum_{j=1}^{J} \lambda_{ex}^{i,j} p_{ex}^{i,j} \Delta \mathrm{T} = \sum_{j=1}^{J} \lambda_{ex,b}^{i,j} p_{ex}^{i,j} \Delta \mathrm{T}. \tag{A1}$$

At the same time, given that $p_{ex}^{i,j} \geq 0$, based on (39), there is

$$\begin{aligned} & M_{ex}^{opr,i} \\ &= \sum_{j=1}^{J} \frac{\Delta \mathrm{T}}{2} \left(\left(\lambda_{ex,b}^{i,j} - \lambda_{ex,s}^{i,j} \right) \left| p_{ex}^{i,j} \right| + \left(\lambda_{ex,b}^{i,j} + \lambda_{ex,s}^{i,j} \right) p_{ex}^{i,j} \right) \\ &= \sum_{j=1}^{J} \frac{\Delta \mathrm{T}}{2} \left(\left(\lambda_{ex,b}^{i,j} - \lambda_{ex,s}^{i,j} \right) p_{ex}^{i,j} + \left(\lambda_{ex,b}^{i,j} + \lambda_{ex,s}^{i,j} \right) p_{ex}^{i,j} \right) \\ &= \sum_{j=1}^{J} \frac{\Delta \mathrm{T}}{2} \left(2 \lambda_{ex,b}^{i,j} p_{ex}^{i,j} \right) \\ &= \sum_{j=1}^{J} \lambda_{ex,b}^{i,j} p_{ex}^{i,j} \Delta \mathrm{T}. \end{aligned} \tag{A2}$$

Comparing (A1) and (A2), it can be seen that $M_{ex}^{opr,i}$ has the exactly same expression, showing that (39) is equivalent to (37) with (38) when $p_{ex}^{i,j} \geq 0$.

For the second part of the proof, when $p_{ex}^{i,j} < 0$, based on (37) and (38), there is

$$M_{ex}^{opr,i} = \sum_{j=1}^{J} \lambda_{ex}^{i,j} p_{ex}^{i,j} \Delta \mathrm{T} = \sum_{j=1}^{J} \lambda_{ex,s}^{i,j} p_{ex}^{i,j} \Delta \mathrm{T}. \tag{A3}$$

At the same time, given that $p_{ex}^{i,j} < 0$, based on (39), there is

$$\begin{aligned} & M_{ex}^{opr,i} \\ &= \sum_{j=1}^{J} \frac{\Delta \mathrm{T}}{2} \left(\left(\lambda_{ex,b}^{i,j} - \lambda_{ex,s}^{i,j} \right) \left| p_{ex}^{i,j} \right| + \left(\lambda_{ex,b}^{i,j} + \lambda_{ex,s}^{i,j} \right) p_{ex}^{i,j} \right) \\ &= \sum_{j=1}^{J} \frac{\Delta \mathrm{T}}{2} \left(\left(\lambda_{ex,b}^{i,j} - \lambda_{ex,s}^{i,j} \right) \left(-p_{ex}^{i,j} \right) + \left(\lambda_{ex,b}^{i,j} + \lambda_{ex,s}^{i,j} \right) p_{ex}^{i,j} \right) \\ &= \sum_{j=1}^{J} \frac{\Delta \mathrm{T}}{2} \left(2 \lambda_{ex,s}^{i,j} p_{ex}^{i,j} \right) \\ &= \sum_{j=1}^{J} \lambda_{ex,s}^{i,j} p_{ex}^{i,j} \Delta \mathrm{T}. \end{aligned} \tag{A4}$$

Comparing (A3) and (A4), it can be seen that $M_{ex}^{opr,i}$ has the exactly same expression, showing that (39) is equivalent to (37) with (38) when $p_{ex}^{i,j} < 0$.

Combining the conclusions of the two parts of the proof, it is proved that (39) is equivalent to (37) with (38).

B. PROOF OF EQ. (40) With EQ. (41) BEING EQUIVALENT TO EQ. (39)

In this section, it will be further proved that (40) with (41) is equivalent to (39). The proof also includes two parts.

For the first part of the proof, when $p_{ex}^{i,j} > 0$, based on (41), there is

$$g_s^j = p_{ex}^{i,j}. \tag{A5}$$

To derive (A5) from (41), it is important to note that for g_b^j and g_s^j, at least one of them equals to 0. This is because that the $M_{ex}^{opr,i}$ expressed in (40) is minimized in the objective function [see (12) and (16)], and if both g_b^j and g_s^j are not equal to zero, the $M_{ex}^{opr,i}$ cannot be minimized. The principles behind this conclusion have been described in other existing studies, such as in Appendix B of [27], as well. With this conclusion, if $g_s^j = 0$, then according to (41), there is $g_b^j = -p_{ex}^{i,j} < 0$, but this is contradictory to $g_b^j \geq 0$. Therefore, it is g_b^j that equals to 0. Substituting $g_b^j = 0$ into (41), (A5) is obtained.

Substituting (A5) and $g_b^j = 0$ into (40), there is

$$\begin{aligned} M_{ex}^{opr,i} &= \sum_{j=1}^{J} \frac{\Delta \mathrm{T}}{2} \left(\left(\lambda_{ex,b}^{i,j} - \lambda_{ex,s}^{i,j} \right) \left(g_b^j + g_s^j \right) \right. \\ &\quad \left. + \left(\lambda_{ex,b}^{i,j} + \lambda_{ex,s}^{i,j} \right) p_{ex}^{i,j} \right) \\ &= \sum_{j=1}^{J} \frac{\Delta \mathrm{T}}{2} \left(\left(\lambda_{ex,b}^{i,j} - \lambda_{ex,s}^{i,j} \right) \left(0 + p_{ex}^{i,j} \right) \right. \\ &\quad \left. + \left(\lambda_{ex,b}^{i,j} + \lambda_{ex,s}^{i,j} \right) p_{ex}^{i,j} \right) \\ &= \sum_{j=1}^{J} \frac{\Delta \mathrm{T}}{2} \left(2 \lambda_{ex,b}^{i,j} p_{ex}^{i,j} \right) \\ &= \sum_{j=1}^{J} \lambda_{ex,b}^{i,j} p_{ex}^{i,j} \Delta \mathrm{T}. \end{aligned} \tag{A6}$$

Comparing (A6) and (A2), it can be seen that $M_{ex}^{opr,i}$ has the exactly same expression, showing that (40) with (41) is equivalent to (39) when $p_{ex}^{i,j} > 0$.

Following the similar procedure, it is easy to derive that (40) with (41) is also equivalent to (39) when $p_{ex}^{i,j} \leq 0$. Therefore, it is proved that (40) with (41) is equivalent to (39).

REFERENCES

[1] Y. Li, Y. Li, G. Li, D. Zhao, and C. Chen, "Two-stage multi-objective OPF for AC/DC grids with VSC-HVDC: Incorporating decisions analysis into optimization process," *Energy*, vol. 147, pp. 286–296, Mar. 2018.

[2] L. Che, M. Shahidehpour, A. Alabdulwahab, and Y. Al-Turki, "Hierarchical coordination of a community microgrid with AC and DC microgrids," *IEEE Trans. Smart Grid*, vol. 6, no. 6, pp. 3042–3051, Nov. 2015.

[3] X. Jin, J. Wu, Y. Mu, M. Wang, X. Xu, and H. Jia, "Hierarchical microgrid energy management in an office building," *Appl. Energy*, vol. 208, pp. 480–494, Dec. 2017.

[4] D. Zhang, N. Shah, and L. G. Papageorgiou, "Efficient energy consumption and operation management in a smart building with microgrid," *Energy Convers. Manage.*, vol. 74, pp. 209–222, Oct. 2013.

[5] M. Gheydi, A. Nouri, and N. Ghadimi, "Planning in microgrids with conservation of voltage reduction," *IEEE Syst. J.*, vol. 12, no. 3, pp. 2782–2790, Sep. 2018.

[6] Y. Li, Z. Yang, G. Li, Y. Mu, D. Zhao, C. Chen, and B. Shen, "Optimal scheduling of isolated microgrid with an electric vehicle battery swapping station in multi-stakeholder scenarios: A bi-level programming approach via real-time pricing," *Appl. Energy*, vol. 232, pp. 54–68, Dec. 2018.

[7] M. Quashie, F. Bouffard, C. Marnay, R. Jassim, and G. Joós, "On bilevel planning of advanced microgrids," *Int. J. Elect. Power Energy Syst.*, vol. 96, pp. 422–431, Mar. 2018.

[8] Y. Zhang, J. Wang, A. Berizzi, and X. Cao, "Life cycle planning of battery energy storage system in off-grid wind–solar–diesel microgrid," *IET Gener., Transmiss. Distrib.*, vol. 12, no. 20, pp. 4451–4461, Nov. 2018.

[9] I. Alsaidan, A. Khodaei, and W. Gao, "A comprehensive battery energy storage optimal sizing model for microgrid applications," *IEEE Trans. Power Syst.*, vol. 33, no. 4, pp. 3968–3980, Jul. 2018.

[10] J. Mitra, M. R. Vallem, and C. Singh, "Optimal deployment of distributed generation using a reliability criterion," *IEEE Trans. Ind. Appl.*, vol. 52, no. 3, pp. 1989–1997, May/Jun. 2016.

[11] S. C. Madathil, E. Yamangil, H. Nagarajan, A. Barnes, R. Bent, S. Backhaus, S. J. Mason, S. Mashayekh, and M. Stadler, "Resilient off-grid microgrids: Capacity planning and N-1 security," *IEEE Trans. Smart Grid*, vol. 9, no. 6, pp. 6511–6521, Nov. 2018.

[12] A. Kumar, A. R. Singh, Y. Deng, X. He, P. Kumar, and R. C. Bansal, "A novel methodological framework for the design of sustainable rural microgrid for developing nations," *IEEE Access*, vol. 6, pp. 24925–24951, 2018.

[13] M. Nasir, S. Iqbal, and H. A. Khan, "Optimal planning and design of low-voltage low-power solar DC microgrids," *IEEE Trans. Power Syst.*, vol. 33, no. 3, pp. 2919–2928, May 2018.

[14] E. Hajipour, M. Bozorg, and M. Fotuhi-Firuzabad, "Stochastic capacity expansion planning of remote microgrids with wind farms and energy storage," *IEEE Trans. Sustain. Energy*, vol. 6, no. 2, pp. 491–498, Apr. 2015.

[15] C. Zhang, Y. Xu, and Z. Y. Dong, "Probability-Weighted robust optimization for distributed generation planning in microgrids," *IEEE Trans. Power Syst.*, vol. 33, no. 6, pp. 7042–7051, Nov. 2018.

[16] S. Bahramirad, W. Reder, and A. Khodaei, "Reliability-constrained optimal sizing of energy storage system in a microgrid," *IEEE Trans. Smart Grid*, vol. 3, no. 4, pp. 2056–2062, Dec. 2012.

[17] X. Cao, J. Wang, and B. Zeng, "A chance constrained information-gap decision model for multi-period microgrid planning," *IEEE Trans. Power Syst.*, vol. 33, no. 3, pp. 2684–2695, May 2018.

[18] S. Mashayekh, M. Stadler, G. Cardoso, M. Heleno, S. C. Madathil, H. Nagarajan, R. Bent, M. Mueller-Stoffels, X. Lu, and J. Wang, "Security-constrained design of isolated multi-energy microgrids," *IEEE Trans. Power Syst.*, vol. 33, no. 3, pp. 2452–2462, May 2018.

[19] A. Khodaei, S. Bahramirad, and M. Shahidehpour, "Microgrid planning under uncertainty," *IEEE Trans. Power Syst.*, vol. 30, no. 5, pp. 2417–2425, Sep. 2015.

[20] R. Rigo-Mariani, B. Sareni, and X. Roboam, "Integrated optimal design of a smart microgrid with storage," *IEEE Trans. Smart Grid*, vol. 8, no. 4, pp. 1762–1770, Jul. 2017.

[21] M. Arriaga, C. A. Cañizares, and M. Kazerani, "Long-term renewable energy planning model for remote communities," *IEEE Trans. Sustain. Energy*, vol. 7, no. 1, pp. 221–231, Jan. 2016.

[22] S. Mohamed, M. F. Shaaban, M. Ismail, E. Serpedin, K. A. Qaraqe, "An efficient planning algorithm for hybrid remote microgrids," *IEEE Trans. Sustain. Energy*, vol. 10, no. 1, pp. 257–267, Jan. 2017.

[23] Jiangsu Development & Reform Commission. (Mar. 2018). *Guidance on Promoting the Development of Distributed Energy Microgrids*. [Online]. Available: http://fzggw.jiangsu.gov.cn/art/2018/3/28/art_51012_7661673.html

[24] R. Carli, M. Dotoli, "Decentralized control for residential energy management of a smart users' microgrid with renewable energy exchange," *IEEE/CAA J. Automatica Sinica*, vol. 6, no. 3, pp. 641–656, May 2019.

[25] Y. M. Atwa, E. F. El-Saadany, M. M. A. Salama, and R. Seethapathy, "Optimal renewable resources mix for distribution system energy loss minimization," *IEEE Trans. Power Syst.*, vol. 25, no. 1, pp. 360–370, Feb. 2010.

[26] S. M. Hosseini, R. Carli, and M. Dotoli, "Model predictive control for real-time residential energy scheduling under uncertainties," in *Proc. IEEE Int. Conf. Syst., Man, Cybern. (SMC)*, Miyazaki, Japan, Oct. 2018, pp. 1386–1391.

[27] C. Wang, Y. Zhou, B. Jiao, Y. Wang, W. Liu, and D. Wang, "Robust optimization for load scheduling of a smart home with photovoltaic system," *Energy Convers. Manage.*, vol. 102, pp. 247–257, Sep. 2015.
[28] L. Guo, W. Liu, B. Jiao, B. Hong, and C. Wang, "Multi-objective stochastic optimal planning method for stand-alone microgrid system," *IET Gener., Transmiss. Distrib.*, vol. 8, no. 7, pp. 1263–1273, Jul. 2014.

QIFANG CHEN (S'13–M'17) received the B.S. and M.S. degrees in communication engineering and electric engineering from Xiangtan University, Hunan, in 2010 and 2013, respectively, and the Ph.D. degree in electrical engineering from North China Electric Power University, Beijing, China, in 2017. He is currently a Postdoctoral Researcher with the School of Electrical Engineering, Beijing Jiaotong University, Beijing. He is also an Academic Visitor with the School of Engineering, Cardiff University, Cardiff, U.K. His research interests include integrated energy system, demand response, and flexible load modeling and control.

MINGCHAO XIA (M'03–SM'17) received the B.S. and Ph.D. degrees in electrical engineering from Tsinghua University, Beijing, China, in 1998 and 2003, respectively. He is currently a Professor with the School of Electrical Engineering, Beijing Jiaotong University. His current research interests include energy Internet, smart power distribution system control and optimization, power electronics in power distribution, and flexible load control.

YUE ZHOU (M'13) received the B.S., M.S., and Ph.D. degrees in electrical engineering from Tianjin University, Tianjin, China, in 2011, 2016, and 2016, respectively. He is currently a Postdoctoral Research Associate with the School of Engineering, Cardiff University, Cardiff, U.K. His research interests include demand response, peer-to-peer energy trading, and block chain technology.

HANMIN CAI received the M.Sc. degree in electrical and electronic engineering from École Polytechnique Fédérale de Lausanne (EPFL), Switzerland, in 2015. He is currently pursuing the Ph.D. degree with the Center for Electric Power and Energy, Department of Electrical Engineering, Technical University of Denmark, Kongens Lyngby, Denmark. His Ph.D. project interests include integrated demand response to support combined heat and power system operation.

JIANZHONG WU (M'04) received the B.S., M.S., and Ph.D. degrees in electrical engineering from Tianjin University, China, in 1999, 2002, and 2004, respectively.

From 2004 to 2006, he was a Postdoctoral with Tianjin University, China. From 2006 to 2008, he was a Research Fellow with The University of Manchester, U.K. He joined Cardiff University as a Lecturer in 2008, a Senior Lecturer in 2013, a Reader in 2014, and a Professor in 2015. He is currently a Professor of multi-vector energy systems and the Head of Department of Electrical and Electronic Engineering, Cardiff University, U.K. His research interests include energy infrastructure and smart grid.

Prof. Wu is also the Director of Applied Energy UNiLAB on Synergies between Energy Networks. He is also a Co-Director of EPSRC Supergen Energy Networks Hub, and a Co-Director of the U.K. Energy Research Centre. He is also a Subject Editor of applied energy.

HAIBO ZHANG (M'16) was born in Heilongjiang, China, in 1975. He received the Ph.D. degree from the Department of Electrical Engineering, Tsinghua University, Beijing, China, in 2005. He is currently a Professor with North China Electric Power University, Beijing. His research interests include energy management systems and power system simulation and control.